Hydraulic characterization of Pwales aquifer in Malta Island preparatory for planning managed aquifer recharge (MAR) pilot plant

Caratterizzazione idraulica dell'acquifero di Pwales nell'isola di Malta propedeutica alla progettazione di un impianto pilota di ricarica artificiale (MAR)

Maria Clementina CAPUTO[a] ✉ , Lorenzo DE CARLO[a], Antonietta Celeste TURTURRO[a], Manuel SAPIANO[b], Julian MAMO[b,c], Oriana BALZAN[b], Luke GALEA[b], Michael SCHEMBRI[b]

[a] National Research Council (CNR), Water Research Institute (IRSA), Bari, Italy - email ✉ : *maria.caputo@ba.irsa.cnr.it*
email: *celeste.turturro@ba.irsa.cnr.it - lorenzo.decarlo@ba.irsa.cnr.it*

[b] Energy and Water Agency (EWA), Malta - email: *manuel.sapiano@gov.mt; julian.a.mamo@um.edu.mt; oriana.balzan@gov.mt; luke.j.galea@gov.mt; michael.schembri@gov.mt*

[c] Institute of Earth Systems, University of Malta

Correspondence to:
Maria Clementina Caputo ✉
maria.caputo@ba.irsa.cnr.it

Riassunto

Al fine di soddisfare il crescente fabbisogno di acqua per vari scopi, incrementando la disponibilità della risorsa idrica e, principalmente, per soddisfare la domanda di acqua di irrigazione di buona qualità per l'agricoltura, l'Agenzia per l'Energia e l'Acqua di Malta sta progettando di realizzare un impianto pilota di ricarica artificiale dell'acquifero nella Valle di Pwales per migliorare lo stato quantitativo e qualitativo del corpo idrico sotterraneo. A tale scopo è stata effettuata una dettagliata caratterizzazione idraulica della valle i cui risultati sono presentati in questo lavoro.

Nello specifico, le proprietà idrauliche delle rocce che costituiscono l'acquifero di Pwales sono state determinate sia mediante test di laboratorio su campioni, sia attraverso prove di campo effettuate nell'area di studio.

Le funzioni di ritenzione idrica e di conducibilità idraulica, che mettono in relazione rispettivamente il potenziale matriciale, ψ, e la conducibilità idraulica, K, con il contenuto di acqua, θ, sono state misurate utilizzando tre diversi metodi sperimentali, ciascuno dei quali ha consentito di ottenere informazioni in uno specifico range di umidità.

In particolare, le funzioni di ritenzione idrica e di conducibilità idraulica sono state determinate su campioni estratti da blocchi provenienti da tre diverse cave: Ghian Tuffieha, Mellieha e San Martin tutte appartenenti alla formazione denominata Upper Coralline Limestone, che costituisce la zona insatura e ospita la falda idrica sotterranea (zona critica). I dati misurati sperimentalmente, attraverso il software LABROS SoilView Analysis, hanno consentito di parametrizzare le funzioni di ritenzione idrica e conducibilità idraulica, fondamentali per modellare i processi di flusso e trasporto dell'acqua nella zona vadosa.

E' stato effettuato, inoltre, un test infiltrometrico per determinare la conducibilità idraulica satura di campo, K_{fs}, e la velocità d'infiltrazione media.

La conoscenza delle caratteristiche idrauliche dell'acquifero, del tutto assenti nella letteratura scientifica, consentirà di sviluppare un modello numerico sito specifico del flusso delle acque sotterranee al fine di descrivere, comprendere e visualizzare diversi scenari ambientali nonché i potenziali effetti dell'impianto di ricarica artificiale sull'acquifero costiero di Pwales.

Abstract

Whitin the aim to reduce the water demand by increasing water use efficiency and providing alternative water resources, and mainly to meet the demand of good quality irrigation water for agriculture, the Energy and Water Agency of Malta is planning to develop a Managed Aquifer Recharge pilot plant in Pwales Valley to improve the quantitative and qualitative status of the groundwater body. For this reason a detailed hydraulic characterization of the valley was carried out. Specifically, hydraulic properties of the rocks that constitute strata atop of the Pwales aquifer were determined by means of both laboratory measurements on samples and field test carried out in the studied area.

The water retention and hydraulic conductivity functions, which relate the matric potential, ψ, and hydraulic conductivity, K, to the water content, θ, respectively, were measured using three experimental methods because each of them allows to obtain data points in a specific wet range.

The water retention and hydraulic conductivity functions were measured on samples extracted from blocks of Upper Coralline Limestone formation, that hosts the aquifer, collected in three different quarries: Ghian Tuffieha, Mellieha and San Martin areas. The measured water retention and hydraulic conductivity data were fitted with LABROS SoilView Analysis software that allows to describe the functions and obtain the parameters which are crucial for modelling the water flow and transport processes in the critical zone.

In addition, large ring infiltrometer test was carried out to determine the field saturated hydraulic conductivity, K_{fs}, and the average infiltration rate.

Knowledge of the hydraulic characteristics of the Upper Coralline Limestone, completely missing in the scientific literature, allows developing a local groundwater-flow numerical model in order to better describe and understand how the water flows from the soil to the groundwater of the valley and visualize different environmental scenarios such as the potential effects of Managed Aquifer Recharge plant in the Pwales Coastal Groundwater Body.

Introduction

Groundwater has been a major source for meeting domestic, agricultural, and industrial water demands in many countries (United Nations, 2022). However, the salinization of groundwater is a serious concern in assuring the distribution of groundwater supplies, particularly in arid and semi-arid regions (Etikala et al., 2021; Polemio & Zuffianò, 2020). With time, in coastal regions the fresh groundwater is impacted by increased salinity due to intensive anthropogenic activities, like excessive groundwater pumping, as well as climatic extremes.

Managed Aquifer Recharge (MAR) is a methodology of artificially recharging groundwater to provide solutions for storing freshwater within the subsurface based on region-specific characteristics (Stefan & Ansems, 2018; Zhang et al., 2020; Zuurbier et al., 2014). In coastal regions affected by seawater intrusion the efficient implementation of a MAR scheme to manage the water demands during dry periods must consider factors related with site-selection, plant design and operational management that influence the aquifer storage and recovery (Tiwari et al., 2022).

Particularly, favorable MAR site selection and appropriate design to achieve higher freshwater recovery in saline groundwater regions need detailed investigation of aquifer hydrogeological characteristics such as porosity, hydraulic gradient, hydraulic conductivity, water retention, aquifer thickness and heterogeneity, and groundwater salinity (Khalil et al., 2022). Hydraulic conductivity, combined with hydraulic gradient, governs the flow velocity of the groundwater, consequently, an increase in hydraulic gradient and/or conductivity causes faster movement of the water during injection and recovery phases by inducing fast fresh and saline water mixing and thus reduces the amount of recoverable freshwater. A low influence of hydraulic gradient on recovery efficiency is observed in aquifers with low hydraulic conductivity (Majumdar et al., 2021). Moreover, increasing hydraulic gradient, relied greatly on the regional hydraulic gradient, causes a significant drop in recovery efficiency. Instead, the aquifer porosity, which determines the aquifer storage capacity is inversely related to the recovery efficiency. In fact, higher porosity implies more time to replace brackish groundwater with injected freshwater. Also, the aquifer thickness affects the recovery efficiency (Lowry & Anderson, 2006). The thicker the aquifer, the wider the zone of mixing between fresh and saline water, and the lower the recovery efficiency. The efficiency of MAR is also decreased by aquifer heterogeneity, as the variations of aquifer properties influence the movement and storage of water (Sommer et al., 2013). Lower salinity is associated with higher recovery efficiency, because of the floatation stratification effect (Maliva et al, 2020). In order to design a MAR plant with high recovery efficiency, it is important to consider both the mentioned hydrogeological factors and operational conditions.

The Pwales valley in Malta Island is a clear example of the need to study and analyze the mentioned factors. Indeed, lacking in this area a significant surface water body, groundwater represents a major freshwater resource supplying human needs and those related to irrigation purposes. However, saltwater intrusion, water exploitation by pumping wells, especially during the summer period, together with the groundwater nitrate contamination due to the intensive agricultural activity cause a severe water resource depletion of the Pwales valley, reducing freshwater supplies. In addition, the Mediterranean semi-arid climate, characterized by poor wet winters and very dry summers, increases groundwater intensive exploitation by causing its qualitative and quantitative depletion (Polemio et al., 2019). Moreover, the presence of tourists in all the seasons of the year contributes to intensifying the fresh water needs increasing the groundwater overexploitation.

Within this scenario, the Energy and Water Agency (EWA) of Malta plans to design a pilot MAR scheme in the Pwales valley. In order to design and implement a MAR scheme, a detailed investigation of the hydro-geological characteristics of the study is needed. For this purpose, the hydraulic characterization of the aquifers was implemented in this paper by means of both laboratory and field tests, to allow the definition of a conceptual model and to provide crucial parameters for numerical modelling aimed at the design of a suitable MAR scheme to improve the quality of groundwater and to increase the water availability for agricultural purposes.

Study area

The Maltese archipelago, consisting of three main islands, Malta (246 km^2), Gozo (67 km^2), and Comino (3,5 km^2), and other uninhabited islets, is located in the center of the Mediterranean Sea, about 90 km from the southern Sicily and 320 km from the northern Africa (Lotti et al., 2021; Magri, 2006; Polemio et al., 2019). Malta has an average altitude of 109 m above the sea level and 198 km of coastline.

From the geological viewpoint, Malta is composed of biogenic coarse-grained wackestones and packstones carbonate limestones with minor marls and clays (House et al., 1961). Superficial Pleistocene deposits are limited to few localities. Specifically, the lithostratigraphic succession, starting from the oldest to the youngest formation, is represented by: Lower Coralline Limestone (Oligocene), Globigerina Limestone (Miocene), Blue Clay (Miocene), Greensand (Miocene) and Upper Coralline Limestone (Miocene), the latter outcrops extensively in all islands (Fig. 1). The mentioned sedimentary succession was deposited in marine environments at different depths: some sediments deposited in shallow gulf-type area (Lower Coralline Limestone), others in deeper open marine environments (Globigerina Limestone and Blue Clay) and others in shallow open marine environments (Greensand and Upper Coralline Limestone Formation) (Polemio et al., 2019).

From hydrogeological point of view, Malta Island is characterized by two unconfined carbonate porous and fissured aquifers hosted in the Upper and Lower Coralline Limestones, respectively, separated by the impermeable Blue Clay formation (House et al., 1961; Lotti et al., 2021; Newbery J., 1963; Polemio et al., 2019). Specifically, the first, referred as
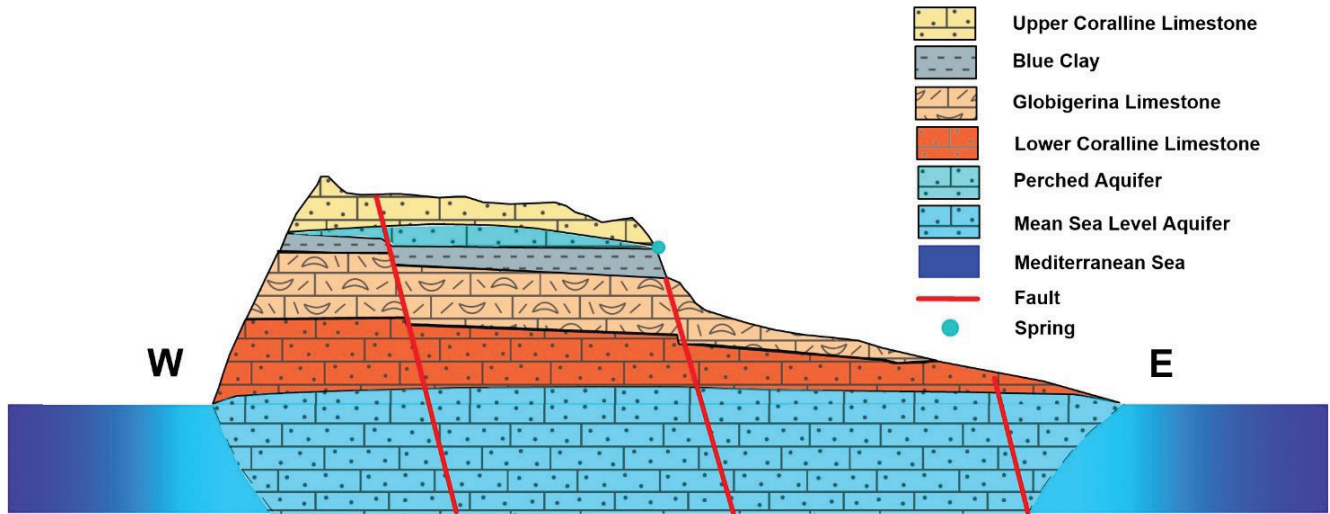
Fig. 1 - *Schematic hydrogeological cross-section from West to East of Malta Island (modified figure from Polemio et al., 2019).*
Fig. 1 - Sezione idrogeologica da ovest a est dell'isola di Malta (figura modificata da Polemio et al., 2019).

the Perched Aquifer, is supported by the Blue Clay formation, while the second, referred as the Mean Sea Level Aquifer, is characterized by a freshwater lens floating over denser seawater (Figure 1). Due to the hydrogeological characteristics, the Mean Sea Level Aquifer is strongly affected by seawater intrusion. Where the bottom of the Upper Coralline Limestone is below the sea-level, the lens-shaped freshwater body also occurs in Upper Coralline Coastal Aquifer. Both aquifers are primarily supplied by rainfall, which infiltrates through fissures and pores of the 50-100 m thick rocky layer in the case of Mean Sea Level Aquifer and 20-50 m thick in the Perched aquifers (Polemio et al., 2019).

This paper is focused on the groundwater of the Pwales coastal aquifer, a part of the Perched Aquifer, that has extremely low-quality conditions as a result of high salinity and nutrient levels caused by seawater intrusion and extensive agricultural activities (Fig. 2).
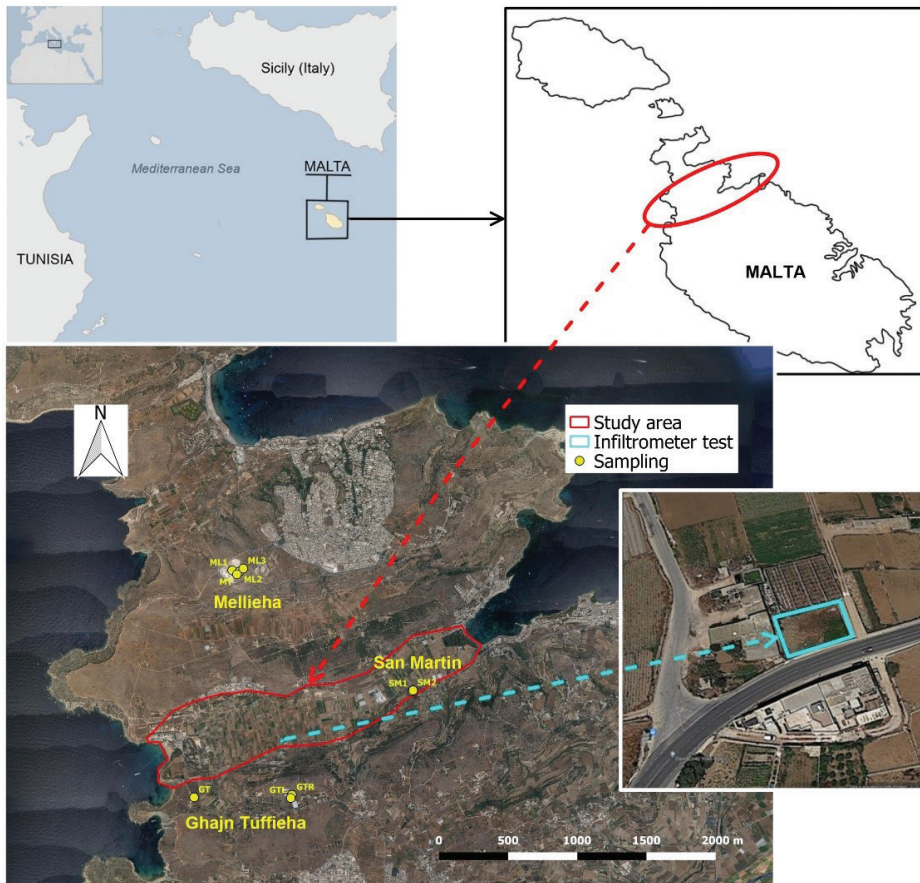
Fig. 2 - *Study area with locations of the Pwales valley limited by the red line, the origins of the samples tested in the laboratory (yellow points), and the infiltrometer test (pale blue line).*
Fig. 2 - Area di studio con la localizzazione della valle Pwales delimitata dalla linea rossa, della provenienza dei campioni analizzati in laboratorio (punti gialli) e della prova infiltrometrica (linea celeste).

Material and Methods

The hydraulic characterization of the studied aquifer was performed by means of both laboratory tests and a field test. Specifically, the laboratory tests were carried out on samples extracted from nine rock blocks coming from three different areas (Ghajn Tuffieha, Mellieha and San Martin) and all belonging to the Upper Coralline Limestone formation (Fig. 3). The field hydraulic characterization was carried out through the infiltrometer test performed in order to obtain the field saturated hydraulic conductivity by installing a large infiltrometer ring on a rocky outcrop (Fig. 4).

Laboratory tests

The samples tested, with specific dimension depending on the used method, were extracted by means of a rotating corer from each of the nine rock blocks and named GT, GTR, GTL, ML1, ML2, ML3, MT, SM1 and SM2, as reported in the Table 1. The rock blocks, 24 x 24 x 15 cm in dimensions, were obtained by cutting using a circular saw from rock boulders coming from Ghajn Tuffieha, Mellieha and San Martin.

Finally, only 7 blocks were tested as it was not possible to extract samples from SM1 and SM2 because of their very crumbly texture. Only the saturated hydraulic conductivity, K_{sat} (m day^{-1}), of the two SM samples was measured as reported in Table 2.

In addition to the physical properties, bulk density, ρ_b (g cm^{-3}), particle density, ρ_p (g cm^{-3}) and porosity, φ, the samples were tested in the laboratory to determine: (i) K_{sat} by means the Falling-Head by Gravity or benchtop method (Klute & Dirksen, 1986); (ii) the water retention curve, by using the suction table (Stackman et al., 1969), Quasi-Steady Centrifuge (QSC) (Caputo & Nimmo, 2005) and psychrometer WP4-T (Andraski & Scanlon, 2002; Campbell et al., 2007) methods; and (iii) the hydraulic conductivity curve measured by using the QSC method.

Tab. 1 - Positions of sampling points of rock blocks from which were extracted the samples investigated in laboratory. The coordinates are expressed in WGS84/UTM33N (EPSG:32633).

Tab. 1 - Posizione dei punti di campionamento dei blocchi di rocce dai quali sono stati estratti i campioni, investigate in laboratorio. Le coordinate sono espresse in WGS84/UTM33N (EPSG:32633).

	Location	Coordinate X	Coordinate Y	Annotation
GT	Ghajn Tuffieha	441163	3976275	
GTR	Ghajn Tuffieha	442313	3976297	
GTL	Ghajn Tuffieha	442300	3976261	
ML1	Mellieha	441630	3978924	First layer from the bottom
ML2	Mellieha	441713	3978908	Second layer from the bottom
ML3	Mellieha	441759	3978944	Third layer from the bottom
MT	Mellieha	441684	3978877	Top layer
SM1	San Martin	443734	3977498	
SM2	San Martin	443745	3977508	

The Falling-Head by Gravity method (Klute & Dirksen, 1986) allowed to measure K_{sat} (m day^{-1}) of samples, 7.8 cm in diameter and 6 cm in height, by applying the relation:

$$K_{sat} = \frac{L}{\Delta t} \ln \frac{H_1}{H_2} \qquad (1)$$

where: L (L) is the sample height, H_1 (L) is the water column height at the start of the test, H_2 (L) is the water column height at the end of the test and Δt (T) is the time required for

GT - Ghajn Tuffieha	MLb1 - Mellieha	SM1 - San Martin
GTr - Ghajn Tuffieha	MLb2 - Mellieha	SM2 - San Martin
GTl - Ghajn Tuffieha	MLb3 - Mellieha	
	MLt - Mellieha	

Fig. 3 - Rock blocks belonging to the Upper Coralline Limestone formation coming from three different areas (Ghajn Tuffieha, Mellieha and San Martin) from which were extracted the samples tested in the laboratory.

Fig. 3 - Blocchi di roccia appartenenti alla formazione del Calcare Corallino Superiore provenienti da tre diverse aree (Ghajn Tuffieha, Mellieha e San Martin) da cui sono stati estratti i campioni testati in laboratorio.

the water level in the reservoir to fall from H_1 to H_2.

The suction table method (Stackman et al., 1969) by using a sandbox (Eijkelkamp Agrisearch Equipment Model 08.01, Ecosearch s.r.l., https://www.royaleijkelkamp.com/media/ny1lqhyr/m-0801e-sandbox-for-pf-determination.pdf) allows to determine the drying water retention curve in a very wet range (ψ between 0 and 2 pF, where pF = - log $|\psi|$, where ψ is expressed in cm). The tested core samples, 3.6 cm in diameter and 5 cm in height, were laterally sealed by using bicomponent transparent epoxy resin (KEMIEPOX 140+EH 248, POOLKEMIE s.r.l.) and saturated under vacuum, successively. A series of static equilibria, between the water inside the samples and a free water body contained in a suction control system at known ψ, were established. For each known ψ value equilibrium was achieved when the sample weight, checked every day, became steady. Hence, the value of θ was determined. Each pair of ψ and θ values identifies an experimental point of the water retention curve.

The psychrometer method (Andraski & Scanlon, 2002; Campbell et al., 2007) uses the WP4-T Decagon Device for measuring water retention curve of rock slices, 0.6 cm in height and 3.6 cm in diameter, in a very dry range. By starting from the initially dry samples, 0.05 g of deionized water was added. When the water content reached the steady state and the water distribution inside the sample was homogeneous, the sample was inserted in the WP4-T device. Once the equilibrium was reached between the liquid-state water in the sample and gas-state water surrounding the sample in a chamber of the device, the latter displays the ψ value based on the Kelvin equation (2)

$$\psi = \left(\frac{RT}{V_w}\right)\ln\left(\frac{p}{p_o}\right) \qquad (2)$$

where R is the universal gas constant ($8.314 \times 10{-}6$ MJ mol^{-1} K^{-1}), T is the temperature (°K), Vw is the molar volume of water (m^3 mol^{-1}), p/p_0 is the relative humidity as a fraction where p (MPa) is the actual vapor pressure of air, in equilibrium with the liquid phase, and p_0 (MPa) is the saturation vapor pressure at T.

Subsequently, the sample was removed from the WP4-T and quickly weighed to determine water content, θ (cm^3 cm^{-3}) by subtracting the dry sample weight to the wet sample weight and dividing it by the sample volume, in order to obtain the pair of values (θ, ψ) of the water retention curve. The procedure is repeated for each water increments until the sample reaches the saturation.

The two methods above mentioned needed to be combined with the Quasi-Steady Centrifuge (QSC) method (Caputo & Nimmo, 2005) in order to describe the entire water retention curve from the very dry range to saturation (Caputo et al., 2022; Turturro et al., 2020; Turturro et al., 2021). The QSC method, by using an experimental apparatus that fits into a swinging centrifuge bucket combined with centrifugal accelerations ranging between 230 and 2000 revolutions

per minute (rpm), allowed measuring of ψ ranging between 1.13 e 2.53 pF, θ between 0.067 and 0.42 cm^3 cm^{-3} and K between 1.29 E-04 and 3.21E-03 m day^{-1}. The upper part of the apparatus rests on the sample and consists of a reservoir which controls the water flow by means of a layer of specific granular material, the conductance of which determines the flow rate. The lower part of the apparatus, located below the sample, includes a ceramic plate placed on the outflow dish, which rests on the bottom of the centrifuge bucket. Once the sample reached the steady-state for specific operational condition, the corresponding ψ value was measured by a contact tensiometer. This method enables the measuring of water retention curve in the whole water content range by simply changing the combination of operative conditions (granular material, speed and run duration) which the flow rate depends on.

The QSC method allowed measuring the hydraulic conductivity curves by computing for each ψ the corresponding K (m day^{-1}) value using the equation (3):

$$q = -k(\theta)\left(\frac{d\psi}{dr} - \rho\omega^2 r\right) \qquad (3)$$

where q is the flux density, ρ is the water density, ω is the angular speed in the centrifuge, r is the distance of the sample center from the rotation axis, K, θ and ψ are already defined.

The measured water retention and hydraulic conductivity data were fitted by applying both the unimodal and bimodal van Genuchten (1980) (vG) and Peters Durner Iden (PDI) (Pertassek et al., 2015) models by using the LABROS SoilView Analysis software (Pertassek et al., 2015).

Field test

For the purpose of this study, the infiltrometer test was carried out on the Upper Coralline limestone Formation outcrop, specifically at the bottom of an infiltration trench located in the Pwales Valley (Fig. 1). This test, that lasted about 2 days including the experimental set-up preparation, measures the field hydraulic conductivity, K_{fs}, of the outcropped rock when it has been brought to a near-saturated state, by using a ring infiltrometer, adjustable in diameter to fit the field condition, such as the lithological and topographical features of the site (Fig. 4). A strip of 60 cm high flexible plastic material was used to build in situ the infiltrometer ring by sealing the two edges with impermeable tape. The ring was installed into about 2 cm deep furrow hollowed in the rock at the bottom of the trench, and sealed with a type of concrete. Although it presents some practical challenges, related to the installation of the ring on the rock surface in order to obtain a continuous and impermeable joint surface between the rock and the ring wall, the infiltrometer test represents an inexpensive and versatile field method for measuring field saturated hydraulic conductivity. Specifically, for this study, a ring with a diameter equal to 1.06 m was installed and the test was performed under falling head

Fig. 4 - Infiltrometer ring installed directly on the outcropped rock at the bottom of the infiltration trench (left); CTD-Diver probe to measure the water level decrease in the ring during the infiltration test (right).

Fig. 2 - Anello infiltrometrico installato direttamente sulla roccia affiorante sul fondo della trincea disperdente (sinistra); sonda CTD-Diver per misurare l'abbassamento del livello d'acqua nell'anello durante il test infiltrometrico (destra).

conditions. About 0.246 m³ of water was poured into the ring until the water level reached about 0.28 m height from its bottom. During the experiments, water level decrease in the ring was monitored by means of a pressure probe, CTD-Diver (CTD-Diver DI28x Series, Ecosearch s.r.l., https://www.vanessen.com/wp-content/uploads/2022/05/CTD-Diver-DI28x-ProductManual-en.pdf) that autonomously measures conductivity, pressure and temperature and records the data in an internal memory. The CTD-Diver sensor was installed at about 0.13 m from the bottom of the ring, which implied that for water levels lower than 0.13 m the sensor could not read because it was out of the water. In addition, the manual measurements, collected in correspondence of the CTD-Diver position in case of sensor's failure, were consistent with those collected automatically by the probe. However, the data considered in this paper were those recorded by the CTD-Diver probes.

The results of the falling-head infiltration test were analyzed using the simplified equation (4) in Nimmo et al. (2009).

$$K_{fs} = \frac{L_G}{t} \ln\left(\frac{L_G + \lambda + D_o}{L_G + \lambda + D} \right) \qquad (4)$$

where K_{fs} (L T^{-1}) is the field-saturated hydraulic conductivity, t is the time, D_0 and D are the initial and final ponded depths, respectively, $L_G = C_1d + C_2b$ is the ring-installation scaling length, with 0.993 and 0.578 as recommended values for C_1 and C_2, d and b are the ring insertion depth and ring radius, respectively, and λ is an index of how strongly water is driven by capillary forces in a particular medium. In the studied case, λ value equals 0.01 m for the Upper Coralline Limestone, taking into account that the sensitivity of conductivity calculations to the value of λ is small (Nimmo et al., 2009), and that Elrick et al. (1989) proposed λ value of about 0.08 m suitable for most soils with structural development, 0.03 m for gravelly soils, and 0.25 m for fine-textured soil without macropores.

Results and Discussion
Laboratory tests

The following Table 2 summarizes the physical properties of the samples tested in the laboratory. The measured values are consistent with those reported in the literature. Specifically, the average porosity value computed from the measures

Tab. 2 - Measured physical properties of the investigated samples: bulk density, ρ_b (g cm^{-3}), particle density, ρ_p (g cm^{-3}), and porosity, φ.

Tab. 2 - Proprietà fisiche dei campioni testati: peso dell'unità di volume, ρ_b (g cm^{-3}), peso specifico, ρ_p (g cm^{-3}) e porosità, φ.

Sample	ρ_b (g cm^{-3})	ρ_p (g cm^{-3})	φ
GT	1.66	2.50	0.33
GTR	1.90	2.60	0.27
GTL	1.57	2.62	0.40
ML1	2.09	2.54	0.17
ML2	1.51	2.61	0.42
ML3	1.65	2.63	0.37
MT	1.56	2.66	0.41
SM1	-	-	-
SM2	-	-	-

performed in this study equals 0.33, and is really close to 0.30 which is the value reported in De Biase et al. (2023) the sources of which are Haroon et al. (2021) and Kuang et al. (2020).

The water retention data, measured using different methods, allowed to describe the water retention curves for each of the samples extracted from the 7 rock blocks. The software LABROS SoilView Analysis (Pertassek et al., 2015) accurately fitted the experimental data and provided the fitting parameters, crucial for modelling water flow and transport in the vadose zone. Both the unimodal and bimodal van Genuchten (1980) and Peters Durner Iden (Pertassek et al., 2015) models were applied. However, the best fitting of the water retention data was obtained by applying the bimodal Peters-Durner-Iden model that showed root mean square error (RMSE) values lower than the other models ranging

Tab. 3 - *Water retention curves parameters:* θ_r, *residual water content, and* θ_s, *saturated water content, both experimentally measured,* α_1, α_2, n_1, n_2, *shape parameters of the water retention function, and RMSE* θ *calculated by applying the bimodal Peters Durner Iden (Pertassek et al., 2015) model to experimental data.*

Tab.3 - Parametri delle curve di ritenzione: θ_r, contenuto d'acqua residuo e θ_s contenuto d'acqua saturo, entrambi misurati sperimentalmente, α_1, α_2, n_1, n_2 parametri di forma della funzione di ritenzione idrica e RMSE θ calcolati applicando il modello bimodale di Peters Durner Iden (Pertassek et al., 2015) ai dati misurati sperimentalmente.

Sample	θ_r* (cm^3 cm^{-3})	θ_s* (cm^3 cm^{-3})	α_1 (cm^{-1})	α_2 (cm^{-1})	n_1	n_2	RMSE θ
GT	0.001	0.50	0.0757	0.00067	15	1.716	0.0038
GTR	0.001	0.33	0.0301	0.50	15	1.254	0.0267
GTL	0.001	0.33	0.50	0.0281	1.268	15	0.0247
ML1	0.001	0.31	0.50	0.0183	15	1.837	0.0198
ML2	0.001	0.35	0.055	0.0313	1.570	15	0.0110
ML3	0.001	0.37	0.50	0.00505	1.388	2.097	0.0158
MT	0.001	0.37	0.00129	0.50	3.877	2.216	0.0286
*values experimentally measured							

from 0.0038 and 0.0267. The parameters of all the fitted water retention curves, that are θ_r, residual water content, and θ_s, saturated water content, α_1, α_2, n_1, n_2, shape parameters of the bimodal Peters-Durner-Iden model (Pertassek et al., 2015), together with the RMSE are listed in Table 3.

The hydraulic conductivity data measured by the QSC method were best fitted by applying the unimodal van Genuchten model using the same software above mentioned. The obtained best fit parameters are listed in Table 4. The unimodal van Genuchten model resulted to be the best fitting model for the experimental data, although RMSE K values ranges between 0 and 0.45 because of the limited number of available experimental data.

Tab. 4 - *Parameters of hydraulic conductivity curves:* θ_r, *residual water content, and* θ_s, *saturated water content, both experimentally measured,* α *and n, shape parameters of the hydraulic conductivity function, and RMSE K calculated by applying the unimodal van Genuchten (van Genuchten, 1980) model to the experimental data, and saturated hydraulic conductivity, Ksat measured by using the falling-head by gravity method (Klute & Dirksen, 1986).*

Tab.4 - Parametri delle curve di conducibilità idraulica: θ_r, contenuto d'acqua residuo e θ_s contenuto d'acqua saturo, entrambi misurati sperimentalmente, α, n, parametri di forma della funzione di conducibilità idraulica, e RMSE K calcolati applicando il modello di van Genuchten (van Genuchten, 1980) e valori di conducibilità idraulica satura, K_{sat}, misurati con il metodo a carico variabile (Klute & Dirksen, 1986).

Sample	θ_r* (cm^3 cm^{-3})	θ_s* (cm^3 cm^{-3})	α (cm^{-1})	n (cm^{-1})	RMSE K	K_{sat}
GT	0.001	0.50	0.00144	1.240	0.3562	5.995
GTR	0.001	0.33	0.00001	1.067	0.2758	3.998
GTL	0.001	0.33	0.0175	1.466	0.0000	2.202
ML1	0.001	0.31	0.0182	2.101	0.3839	10.342
ML2	0.001	0.35	0.00951	3.147	0.4510	8.386
ML3	0.001	0.37	0.00001	1.107	0.0555	5.504
MT	0.001	0.37	0.0141	15	0.3014	4.394
SM2	-	-	-	-	-	5.089
*values experimentally measured						

Overall, the hydraulic characterization carried out in laboratory, highlights that the tested samples, belonging all to the Upper Coralline Limestone formation but coming from different quarries, present differences in terms of texture and porosity reflecting the different hydraulic behavior.

The average K_{sat} value computed from the values measured in this study resulted equal to 5.74 m day^{-1} comparable to 4,23 m day^{-1} reported in De Biase et al. (2023) and one order of magnitude lower than 43.2 m day^{-1}, the value mentioned in Lotti et al. (2021). Haroon et al. (2021), instead, found the hydraulic conductivity value of the Upper Coralline Limestone

equal to 4,32 x 10^{-2} m day^{-1}. This value, that is 2-3 orders of magnitude lower than the previous ones, was measured in an area close to Marfa, a location far from the quarries form which the samples tested in this study come from. This fact highlights the strong heterogeneity of the Upper Coralline Limestone formation consistent with the range of values ranging from 8.64 x 10^{-1} to 8.64 x 10^{-4} m day^{-1} reported in Haroon et al. (2021), the sources of which are Bakalowicz and Mangion (2003), Sapiano et al. (2017) and ERA (2015), and those indicated in Demichele et al. (2023) that range from 1.90 x 102 to 1.81 m day^{-1}.

Infiltrometer test

The results of the infiltrometer test are shown in Figure 5. The graph in Figure 5 shows a constant decrease in the water level in the ring during the infiltrometer test, recorded by the CTD-Diver probes, starting from the
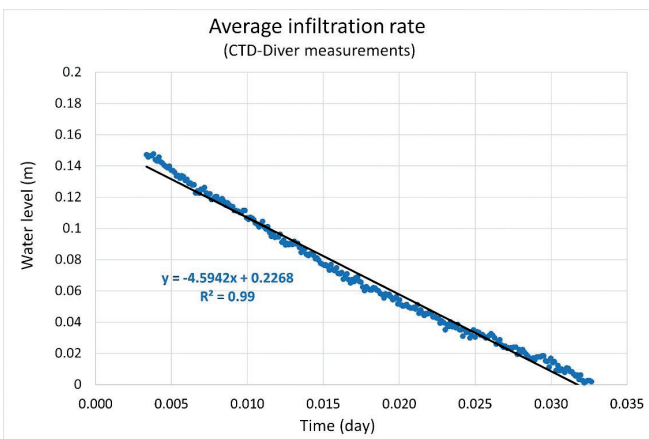
Fig. 5 - Average infiltration rate computed from the measurements of water level decrease recorded, by means the CTD-Diver probe, during the infiltrometer test.

Fig. 5 - Velocità di infiltrazione media calcolata dall'abbassamento del livello dell'acqua registrato, attraverso la sonda CTD-Diver, durante il test infiltrometrico.

maximum water level of about 0.28 m from the bottom of the trench that corresponds to 0.15 m in the graph. It is important to highlight that the value 0 of water level for the CTD-Diver measurements corresponds to about 13 cm from the bottom of the infiltrometer ring. The slope of the trend line shown in the graph of Figure 5 represents the average infiltration rate that is of about 4.6 m day^{-1}.

The plot of the effective infiltration length (right-hand side of the equation 4 except for variable t) vs. time in Figure 6 is a useful method for calculating K_{fs}. The graph
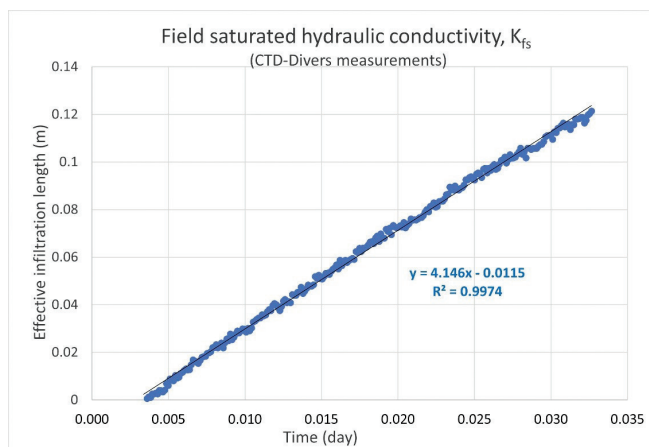
Fig. 6 - Field hydraulic conductivity computed from the measurements of water level decrease recorded, by means the CTD-Diver probe, during the infiltrometer test.

Fig. 6 - Conducibilità idraulica di campo calcolata dalle misure di abbassamento del livello dell'acqua registrate, mediante la sonda CTD-Diver, durante il test infiltrometrico.

shows the K_{fs} value obtained from the elaboration of the measurements collected from the CTD-Diver probe equal to 4.15 m day^{-1}. The results obtained from infiltrometer test highlighted that the field saturated hydraulic conductivity values are of the same order of magnitude than the saturated hydraulic conductivity values measured in the laboratory on the core samples by using the Falling-Head by Gravity method.

The infiltrometer test proved to be an effective tool to determine how fast the water flows in the subsoil. Although there are some practical challenges to install the ring on the rock surface, mainly related to the good sealing of the ring to the outcropping rock, in order to achieve a continuous and impermeable joint surface between the rock and the ring wall. The infiltrometer test is a cost-effective and versatile field method for measuring saturated hydraulic conductivity. For above mentioned reasons, the infiltrometer test is strongly suggested to be performed at the bottom of other trenches planned to be used as part of a MAR scheme, although it implies to face site specific aspects that need to be solved each time to have accurate results.

Conclusion

The paper presents the results of the hydraulic characterization of the Upper Coralline Limestone formation that hosts the coastal aquifer of Pwales Valley in Malta island where the Energy and Water Agency (EWA) of Malta plans to design a MAR pilot scheme. Due to the absence of scientific data on the hydraulic properties of the aquifer, laboratory tests were conducted on samples collected from nine different locations, all of which belong to the same geological formation, as well as field infiltration test. Specifically, the experimental data obtained using three different laboratory methods, were fitted by using the software LABROS SoilView Analysis. The fitting produced water retention and hydraulic conductivity curves together with their equations parameters, crucial parameters for modelling water flow and transport in the vadose zone. Overall, the bimodal Peters-Durner-Iden model best fitted the water retention data while the unimodal van Genuchten model worked well to fit the hydraulic conductivity curves.

The model equations, commonly used to describe unsaturated flow, provided parameters which are essential for modelling the flow in the vadose zone, therefore essential for designing the MAR plant.

In detail, the experimental data obtained in laboratory highlight that the samples, even if they belong all to same geological formation (Upper Coralline Limestone Formation) differ in their hydraulic behavior such as in texture and porosity. By comparing laboratory and field measurements it arises that saturated hydraulic conductivity values measured in laboratory are of the same order of magnitude of field saturated hydraulic conductivity value derived by field infiltration test (5 m day^{-1}).

The results of this study provide crucial outcomes because are experimentally obtained and provide information,

specifically referred to hydraulic conductivity and water retention functions completely missing in the scientific literature. Particularly, the site specific hydraulic characteristic functions, obtained through several laboratory tests and field infiltrometer test, constitute a preliminary but essential data base to implement a detailed numerical model in order to simulate the real behavior of the Pwales coastal groundwater body, and create a hydrological model, at catchment scale, preparatory to designing MAR plant. This will be the most important benefit of the study's outcomes: it will provide a very helpful support for the decision makers of the Energy and Water Agency of Malta.

Competing interest
All authors, declare no competing interests.

Author contributions
Collection of data, Maria C. Caputo, Lorenzo De Carlo, Antonietta C. Turturro, Luke Galea, Oriana Balzan, Michael Schembri; data processing, Maria C. Caputo, Antonietta C. Turturro; interpretation of results, Maria C. Caputo, Antonietta C. Turturro; writing-original draft preparation, Maria C. Caputo, Antonietta C. Turturro; writing-review and editing, Maria C. Caputo, Antonietta C. Turturro, Julian Mamo; visualization, Maria C. Caputo, Antonietta C. Turturro; supervision, Maria C. Caputo, Lorenzo De Carlo, Manuel Sapiano, Michael Schembri; project administration, Maria C. Caputo, Lorenzo De Carlo, Manuel Sapiano. All authors have read and agreed to the final version of the manuscript.

Additional information
DOI: https://doi.org/10.7343/as-2024-742
Reprint and permission information are available writing to acquesotterranee@anipapozzi.it
Publisher's note Associazione Acque Sotterranee remains neutral with regard to jurisdictional claims in published maps and institutional affiliations.

REFERENCES

Andraski, B. J., & Scanlon, B. R. (2002). Thermocouple Psychrometry. In Physical Methods of Soil Analysis 4 (pp. 609-615). SSSA BOOK SERIES:5

Bakalowicz, M., & Mangion, J. (2003). The limestone aquifers of Malta: Their recharge conditions from isotope and chemical surveys. Paper presented at the Hydrology of the Mediterranean and Semiarid Regions, Proceedings of an International Symposium held at Montpellier. IAHS. No. 278.

Campbell, G. S., Smith, D. M., & Teare, B. L. (2007). Application of a dew point method to obtain the soil water characteristic. In Experimental unsaturated soil mechanics (pp. 71– 77).

Caputo, M. C., De Carlo, L., Masciopinto, C., & Nimmo, J. R. (2010). Measurement of field-saturated hydraulic conductivity on fractured rock outcrops near Altamura (Southern Italy) with an adjustable large ring infiltrometer. Environmental Earth Sciences, 60, 583-590. https://doi 10.1007/s12665-009-0198-y

Caputo, M. C., De Carlo, L., & Turturro, A. C. (2022). HYPROP-FIT to model rock water retention curves estimated by different methods. Water, 14, 3443. https:// doi.org/10.3390/w14213443

Caputo, M. C., & Nimmo, J. R. (2005). Quasi-steady centrifuge method of unsaturated hydraulic properties. Water Resources Research, 41, 1-5. https://doi: 10.1029/2005WR003957

De Biase, M., Chidichimo, F., Micallef, A., Cohen, D., Gable, C., & Zwinger, T. (2023). Past and future evolution of the onshore-offshore groundwater system of a carbonate archipelago: The case of the Maltese Islands, central Mediterranean Sea. Frontiers in Water, 4,1068971. https://doi: 10.3389/frwa.2022.1068971

Demichele, F., Micallef, F., Portoghese, I., Mamo, J.A., Sapiano, M., Schembri, M. & Schüth, C. (2023). Determining Aquifer Hydrogeological Parameters in Coastal Aquifers from Tidal Attenuation Analysis, Case Study: The Malta Mean Sea Level Aquifer System. Water, 15 (1), 177, 21. https://doi.org/10.3390/w15010177

Elrick, D. E, Reynolds, W. D., & Tan, K. A. (1989). Hydraulic conductivity measurements in the unsaturated zone using improved well analyses. Ground Water Monitoring Review, 9, 184-193.

ERA - Environment and Resources Authority. (2015). The 2nd Water Catchment Management Plan for the Malta Water Catchment District 2015–2021. Sustainable Energy and Water Conservation Unit Environment and Resources Authority.

Etikala, B., Adimalla, N., Madhav, S., Somagouni, S. G., & Keshava Kiran Kumar, P. L. (2021). Salinity problems in groundwater and management strategies in arid and semi-arid regions. Groundwater Geochemistry: Pollution and Remediation Methods, 42–56. https://doi.org/10.1002/9781119709732.ch3

Haroon, A., Micallef, A., Jegen, M., Schwalenberg, K., Karstens, J., Berndt, C., et al. (2021). Electrical resistivity anomalies offshore a carbonate coastline: evidence for freshened groundwater? Geophysical Research Letters, 48, e2020GL091909. https://doi: 10.1029/2020GL091909

House, M. R., Dunham, K. C., & Wigglesworth, J. C. (1961). Geology and structure of the Maltese isalnds. In Malta: Background for Development (pp. 24-33). Durham

Khalil, K., Khan, Q., & Mohamed, M. (2022). Selection criteria of best sites for aquifer storage and recovery in the Eastern District of Abu Dhabi, United Arab Emirates. Groundwater for Sustainable Development, 100771. https://doi.org/10.1016/j.gsd.2022.100771

Klute, A., & Dirksen, C. (1986). Hydraulic conductivity and diffusivity: laboratory methods. In Methods of Soil Analysis 1, edited by A. Klute, Agronomy 9 (pp. 687–732).

Kuang, X., Jiao, J. J., Zheng, C., Cherry, J. A., & Li, H. (2020). A review of specific storage in aquifers. Journal of Hydrology, 581, 124383. https://doi: 10.1016/j.jhydrol.2019.124383

Lotti, F., Borsi, I., Guastaldi, E., Barbagli, A., Basile, P., Favaro, L., Mallia, A., Xuereb, R., Schembri, M., Mamo, J. A., Demichele, F., & Sapiano, M. (2021). NECoM (Numerically Enhanced COnceptual Modelling) of two small Maltese aquifers: Mizieb and Pwales. Acque sotterranee – Italian Journal of Groundwater – AS36-496, 7-21. https://doi 10.7343/as-2021-496

Lowry, C. S., & Anderson, M.P. (2006). An Assessment of Aquifer Storage Recovery Using Ground Water Flow Models. Groundwater, 44, 661-667. https://doi.org/10.1111/j.1745-6584.2006.00237.x

Magri, O. (2006). A geological and geomorfological review of the Meltese islands with special reference to the coastal zone. Territoris, 6, 7-26.

Majumdar, S., Miller, G. R., & Sheng, Z. (2021). Optimizing Multiwell Aquifer Storage and Recovery Systems for Energy Use and Recovery Efficiency. Groundwater, 59, 629-643. https://doi.org/10.1111/gwat.13092

Maliva, R. G., Manahan, W. S., & Missimer, T. M. (2020). Aquifer Storage and Recovery Using Saline Aquifers: Hydrogeological Controls and Opportunities. Groundwater, 58, 1, 9–18. https://doi.org/10.1111/gwat.12962

Newbery, J. (1963). The perched water table in the Upper Limestone Aquifer of Malta. Journal of the Institution of Water Engineers, 22, 551-570.

Nimmo, J. R., Schmidt, K. S., Perkins, K. S., & Stock J. D. (2009). Rapid measurement of field-saturated hydraulic conductivity for areal characterization. Vadose Zone Journal, 8, 142-149.

Pertassek, T., Peters, A., & Durner, W. (2015). HYPROP-FIT Software User's Manual, V.3.0; UMS GmbH: München, Germany; 66 pp.

Polemio, M., & Zuffianò, L. E. (2020). Review of utilization management of groundwater at risk of salinization. Journal of Water Resources Planning and Management, 146(9), 03120002, 1-20. https://doi.org/10.1061/(asce)wr.1943-5452.0001278

Polemio, M., Sapiano, M., Santaloia, F., Basso, A., Dragone, V., De Giorgio, G., Limoni, P., Zuffianò, L. E., John, M., & Schembri, M. (2019). A hydrogeological study to support the optimized management of the main sea level aquifer of the island of Malta. Rendiconti Online della Società Geologica Italiana, 47, 85-89.

Sapiano, M., Schembri, M., Debattista, H., & Theuma, N. (2017). Integrating numerical models in river basin management plans: The FREEWAT project. Water Resources Management, 220, 227-238. https://doi.org/10.2495/WRM170221

Sommer, W., Valstar, J., Van Gaans, P., Grotenhuis, T., & Rijnaarts, H. (2013). The impact of aquifer heterogeneity on the performance of aquifer thermal energy storage. Water Resources Research, 49(12), 8128–8138. https://doi.org/10.1002/2013WR013677

Stackman, W. P., Valk, G. A., & van der Harst, G. G. (1969). Determination of soil moisture retention curves I. ICW Wageningen.

Stefan, C., & Ansems, N. (2018). Web-based global inventory of managed aquifer recharge applications. Sustainable Water Resources Management, 4(2), 153–162. https://doi.org/10.1007/s40899-017-0212-6

Tiwari, S., Yadav, B. K., & Polemio, M. (2022). Performance evaluation of Aquifer Storage and Recovery (ASR) system in saline groundwater regions: impact of operational factors and well design. Journal of Hydrologic Engineering, 27(12), 1-10. https://doi.org/10.1061/(asce)he.1943-5584.0002222

Turturro, A. C., Caputo, M. C., Perkins, K. S., & Nimmo, R. J. (2020). Does the Darcy-Buckingham law apply to flow through unsaturated porous rock? Water, 12, 2668. https://doi:10.3390/w12102668

Turturro, A. C., Caputo, M. C., & Gerke, H. H. (2021). Mercury intrusion porosimetry and centrifuge methods for extended-range retention curves of soil and porous rock samples. Vadose Zone Journal, 21, e20176, 1-11. https://doi: 10.1002/vzj2.20176

United Nations (2022). The United Nations World Water Development Report 2022. Groundwater: Making the invisible visible. In UNESCO, Paris. https://doi.org/10.1111/1740-9713.01654

van Genuchten, M. T. (1980). A Closed-form Equation for Predicting the Hydraulic Conductivity of Unsaturated Soils. Soil Science Society of American Journal, 44, 892–898. https://doi.org/10.2136/sssaj1980.03615995004400050002x

Zhang, H., Xu, Y., & Kanyerere, T. (2020). A review of the managed aquifer recharge: Historical development, current situation and perspectives. Physics and Chemistry of the Earth, 118-119, 102887. https://doi.org/10.1016/j.pce.2020.102887

Zuurbier, K. G., Zaadnoordijk, W. J., & Stuyfzand, P. J. (2014). How multiple partially penetrating wells improve the freshwater recovery of coastal aquifer storage and recovery (ASR) systems: A field and modeling study. Journal of Hydrology, 509, 430-441. https://doi.org/10.1016/j.jhydrol.2013.11.057